Ultrafast Phenomena IV

Proceedings of the Fourth
International Conference
Monterey, California, June 11–15, 1984

Editors: D. H. Auston and K. B. Eisenthal

With 370 Figures

Springer-Verlag
Berlin Heidelberg New York Tokyo 1984

Contents

Part I Generation and Measurement Techniques

The Soliton Laser. By L.F. Mollenauer and R.H. Stolen (With 5 Figures) 2

Soliton Shaping Mechanisms in Passively Mode-Locked Lasers and Negative Group Velocity Dispersion Using Refraction
By O.E. Martinez, J.P. Gordon, and R.L. Fork (With 4 Figures) 7

Compression and Shaping of Femtosecond Pulses
By A.M. Weiner, J.G. Fujimoto, and E.P. Ippen (With 5 Figures) 11

Generation of 0.41-Picosecond Pulses by the Single-Stage Compression of Frequency Doubled Nd:YAG Laser Pulses
By A.M. Johnson, R.H. Stolen, and W.M. Simpson (With 4 Figures) ... 16

Compression of Mode-Locked Nd:YAG Pulses to 1.8 Picoseconds
By B.H. Kolner, J.D. Kafka, D.M. Bloom, and T.M. Baer
(With 3 Figures) 19

Effects of Cavity Dispersion on Femtosecond Mode-Locked Dye Lasers
By S. De Silvestri, P. Laporta, and O. Svelto (With 2 Figures) 23

3 MHz Amplifier for Femtosecond Optical Pulses
By M.C. Downer and R.L. Fork (With 1 Figure) 27

Colliding Pulse Femtosecond Lasers and Applications to the Measurement of Optical Parameters. By J.-C. Diels, W. Dietel, E. Döpel, J. Fontaine, I.C. McMichael, W. Rudolph, F. Simoni, R. Torti, H. Vanherzeele, and B. Wilhelmi (With 5 Figures) 30

High Average Power Mode-Locked Co:MgF_2 Laser. By B.C. Johnson, M. Rosenbluh, P.F. Moulton, and A. Mooradian (With 3 Figures) 35

High Power Picosecond Pulses in the Infrared
By P.B. Corkum (With 4 Figures) 38

Stimulated VUV Radiation from HD Excited by a Picosecond ArF* Laser
By T.S. Luk, H. Egger, W. Müller, H. Pummer, and C.K. Rhodes
(With 1 Figure) 42

Procedure for Calculating Optical Pulse Compression from Fiber-Grating Combinations
By R.H. Stolen, C.V. Shank, and T.W. Tomlinson (With 1 Figure) 46

Generation of Infrared Picosecond Pulses Between 1.2μm and 1.8μm Using a Traveling Wave Dye Laser. By H.-J. Polland, T. Elsaesser, A. Seilmeier, and W. Kaiser (With 3 Figures) 49

A New Picosecond Source in the Vibrational Infrared By A.L. Harris, M. Berg, J.K. Brown, and C.B. Harris(With 2 Figures) 52

Generation of Intense, Tunable Ultrahort Pulses in the Ultraviolet Using a Single Escimer Pump Laser. By S. Szatmári and F.P. Schäfer (With 1 Figure) 56

Travelling Wave Pumped Ultrashort Pulse Distributed Feedback Dye Laser By B. Szabó, B. Rácz, Zs. Bor, B. Nikolaus, and A. Müller (With 2 Figures) 60

Picosecond Pulses from Future Synchrotron-Radiation Sources By R.C. Sah, D.T. Attwood, and A.P. Sabersky (With 2 Figures) 63

High Repetition Rate Production of Picosecond Pulses at Wavelength <250 nm . By D.B. McDonald (With 1 Figure) 66

Ultrafast Self-Phase Modulation in a Colliding Pulse Mode-Locked Ring Dye Laser. By Y. Ishida, K. Naganuma, T. Yajima, and L.H. Lin (With 3 Figures) 69

Electro-Optic Phase-Sensitive Detection of Optical Emission and Scattering. By A.Z. Genack (With 2 Figures) 72

Theoretical Studies of Active, Synchronous, and Hybrid Mode-Locking By J.M. Catherall and G.H.C. New (With 3 Figures) 75

Technique for Highly Stable Active Mode-Locking By D. Cotter (With 3 Figures) 78

Continuous Wave Mode-Locked Nd:Phosphate Glass Laser. By S.A. Strobel, P.-T. Ho, C.H. Lee, and G.L. Burdge (With 3 Figures) 81

Active Mode-Locking Using Fast Electro-Optic Deflector. By A. Morimoto, S. Fujimoto, T. Kobayashi, and T. Sueta (With 5 Figures) 84

Stable Active-Passive Mode Locking of an Nd:Phosphate Glass Laser Using Eastman #5 Saturable Dye By L.S. Goldberg and P.E. Schoen (With 3 Figures) 87

Limits to Pulse Advance and Delay in Actively Modelocked Lasers By R.S. Putnam (With 2 Figures) 90

Novel Method of Waveform Evaluation of Ultrashort Optical Pulses By T. Kobayashi, F.-C. Guo, A. Morimoto, T. Sueta, and Y. Cho (With 6 Figures) 93

Noise in Picosecond Laser Systems: Actively Mode Locked CW Nd^{3+}:YAG and Ar^{+} Lasers Synchronously Pumping Dye Lasers. By T.M. Baer and D.D. Smith (With 4 Figures) 96

High Power, Picosecond Phase Coherent Pulse Sequences by Injection Locking. By F. Spano, F. Loaiza-Lemos, M. Haner, and W.S. Warren (With 2 Figures) 99

Passive Mode-Locking with Reverse Saturable Absorption
By D.J. Harter and Y.B. Band (With 3 Figures) 102

Part II Solid State Physics and Nonlinear Optics

Imaging with Femtosecond Optical Pulses
By M.C. Downer, R.L. Fork, and C.V. Shank (With 1 Figure) 106

Femtosecond Multiphoton Photoelectron Emission from Metals
By J.G. Fujimoto, J.M. Liu, E.P. Ippen, and N. Bloembergen
(With 3 Figures) 111

Time-Resolved Laser-Induced Phase Transformation in Aluminum
By S. Williamson, G. Mourou, and J.C.M. Li (With 3 Figures) 114

Picosecond Photoemission Studies of Laser-Induced Phase Transitions in Silicon. By A.M. Malvezzi, H. Kurz, and N. Bloembergen
(With 3 Figures) 118

Dynamics of Dense Electron-Hole Plasma and Heating of Silicon Lattice Under Picosecond Laser Irradiation. By L.A. Lompré, J.M. Liu, H. Kurz, and N. Bloembergen (With 3 Figures) 122

Dynamics of the Mott Transition in CuCl with Subpicosecond Time Resolution. By D. Hulin, A. Antonetti, L.L. Chase, J. Etchepare, G. Grillon, A. Migus, and A. Mysyrowicz (With 3 Figures) 126

Picosecond Dynamics of Hot Dense Electron-Hole Plasmas in Crystalline and Amorphized Si and GaAs
By P.M. Fauchet, and A.E. Siegman (With 3 Figures) 129

Picosecond Optical Excitation of Phonons in Amorphous As_2Te_3
By C. Thomson, J. Strait, Z. Vardeny, H.J. Maris, J. Tauc, and J.J. Hauser (With 3 Figures) 133

Femtosecond Studies of Intraband Relaxation of Semiconductors and Molecules. By A.J. Taylor, D.J. Erskine, and C.L. Tang
(With 5 Figures) 137

Picosecond Laser Studies of Noneqilibrium Electron Heating in Copper
By G.L. Eesley (With 3 Figures) 143

Picosecond Measurement of Hot Carrier Luminescence in $In_{0.53}Ga_{0.47}As$
By K. Kash and J. Shah (With 3 Figures) 147

Picosecond Carrier Dynamics in Semiconductors
By E.O. Göbel, J. Kuhl, and R. Höger (With 3 Figures) 150

Picosecond Dephasing and Energy Relaxation of Excitons in Semiconductors. By Y. Masumoto (With 6 Figures) 156

Femtosecond Dynamics of Nonequilibrium Correlated Electron-Hole Pair Distributions in Room-Temperature GaAs Multiple Quantum Well Structures. By W.H. Knox, R.L. Fork, M.C. Downer, D.A.B. Miller, D.S. Chemla, C.V. Shank, A.C. Gossard, and W. Wiegmann
(With 1 Figure) 162

Femtosecond Transient Anisotropy in the Absorption Saturation of GaAs
By J.L. Oudar, A. Migus, D. Hulin, G. Grillon, J. Etchepare, and
A. Antonetti (With 2 Figures) 166

Holographic Interferometry Using Twenty-Picosecond UV Pulses to Obtain
Time Resolved Hydro Measurements of Selenium and Gold Plasmas
By G.E. Busch, R.R. Johnson, and C.L. Shepard (With 5 Figures) 170

Temporal Development of Absorption Spectra in Alkali Halide Crystals
Subsequent to Band-Gap Excitation. By W.L. Faust, R.T. Williams,
and B.B. Craig (With 1 Figure) 173

Kinetics of Free and Bound Excitons in Semiconductors
By X.-C. Zhang, Y. Hefetz, and A.V. Nurmikko (With 3 Figures) 176

Determination of Surface Recombination Velocities for CdS Crystals
Immersed in Electrolyte Solutions by a Picosecond Photoluminescence
Technique. By D. Huppert, S. Gottesfeld, Z. Harzion, M. Evenor,
and S. Feldberg (With 1 Figure) 181

Pulsewidth Dependence of Various Bulk Phase Transitions and
Morphological Changes of Crystalline Silicon Irradiated by 1 Micron
Picosecond Pulses. By S.C. Moss, I.W. Boyd, T.F. Boggess, and
A.L. Smirl (With 2 Figures) 184

Subthreshold Picosecond Laser Damage in Silicon Associated with Charge
Emission. By Y.K. Jhee, M.F. Becker, and R.M. Walser
(With 1 Figure) 187

Third-Order Nonlinear Susceptibilities of Dye Solutions Determined by
Non-Phasematched Third Harmonic Generation. By A. Penzkofer and
W. Leupacher (With 1 Figure) 190

Excitation Transport and Trapping in a Two-Dimensional Disordered
System: Cresyl Violet on Quartz. By P. Anfinrud, R.L. Crackel,
and W.S. Struve (With 1 Figure) 193

Temporal Dependence of Third-Order Non-Linear Optical Susceptibilities
of Fused Quartz and Liquid CCl_4. By J. Etchepare, G. Grillon,
I.Thomazeau, J.P. Chambaret, and A. Orszag (With 2 Figures) 196

High Excitation Electron Dynamics in GaInAsP. By A. Miller,
R.J. Manning, A.M. Fox, and J.H. Marsh (With 2 Figures) 199

Picosecond Nonlinear-Optical Limiting in Silicon
By T.F. Boggess, S.C. Moss, I.W. Boyd, and A.L. Smirl
(With 3 Figures) 202

Nonlinear Absorption and Nonlinear Refraction Studies in MEBBA
By M.J. Soileau, W.E. Williams, E.W. Van Stryland, S. Guha,
H. Vanherzeele, J.L.W. Pohlmann, E.J. Sharp, and G.L. Wood
(With 3 Figures) 205

High Density Carrier Generation in Indium Antimonide
By M. Sheikbahae, P. Mukherjee, M. Hasselbeck, and H.S. Kwok 208

Measurement of Two-Photon Cross-Section in DABCO with the Use of Pico-
second Pulses. By G. Arjavalingam, J.H. Glownia, and P.P. Sorokin . 211

Part III Coherent Pulse Propagation

Coherence Effects in Pump-Probe Measurements with Collinear, Copropagating Beams. By S.L. Palfrey, T.F. Heinz, and K.B. Eisenthal (With 2 Figures) 216

Observation of the 0π Pulse. By J.E. Rothenberg, D. Grischkowsky, and A.C. Balant (With 2 Figures) 220

Picosecond Two-Color Photon Echoes in Doped Molecular Solids By D.A. Wiersma, D.P. Weitekamp, and K. Duppen (With 1 Figure) 224

Subpicosecond Accumulated Photon Echoes with Incoherent Light in Nd^{3+}-Doped Silicate Glass. By H. Nakatsuka, S. Asaka, M. Fujiwara, and M. Matsuoka (With 3 Figures) 226

Femtosecond Dephasing Measurements Using Transient Induced Gratings By A.M. Weiner, S. De Silvestri, and E.P. Ippen (With 4 Figures) .. 230

Picosecond Pulse Multiphoton Coherent Propagation in Vapors By H. Vanherzeele, and J.-C. Diels (With 2 Figures) 233

Stimulated Photon Echo for Elastic and Depolarizing Collison Studies By J.-C. Keller and J.-L. Le Gouet (With 3 Figures) 236

Coherent Transient Spectroscopy with Ultra-High Time Resolution Using Incoherent Light. By N. Morita, T. Yajima, and Y. Ishida (With 3 Figures) 239

Part IV Stimulated Scattering

Interaction-Induced, Subpicosecond Phenomena in Liquids By P.A. Madden (With 4 Figures) 244

Transient Infrared Spectroscopy on the Picosecond and Sub-Picosecond Time Scale. By H.-J. Hartmann and A. Laubereau (With 5 Figures) ... 252

Quantum Fluctuations in Picosecond Transient Stimulated Raman Scattering By N. Fabricius, K. Nattermann, and D. von der Linde (With 2 Figures) 258

Transient Coherent Raman Spectroscopy: Two Novel Ways of Line Narrowing By W. Zinth, M.C. Nuss, and W. Kaiser (With 2 Figures) 263

Picosecond Transient Raman Spectroscopy: The Excited State Structure of Diphenylpolyenes. By T.L. Gustafson, D.A. Chernoff, J.F. Palmer, and D.M. Roberts (With 3 Figures) 266

Time-Resolved Nonlinear Spectroscopy of Vibrational Overtones and Two-Phonon States. By G.M. Gale, M.L. Geirnaert, P. Guyot-Sionnest, and C. Flytzanis (With 4 Figures) 270

Direct Picosecond Determination of the Character of Virbrational Line Broadening in Liquids. By G.M. Gale, P. Guyot-Sionnest, and W.Q. Zheng (With 2 Figures) 274

Picosecond Time-Domain Coherent Active Raman Spectroscopy of Free Nitrogen Jet. By S.A. Akhmanov, N.I. Koroteev, S.A. Magnitskii, V.B. Morozov, A.P. Tarassevich, V.G. Tunkin, and I.L. Shumay (With 2 Figures) 278

Part V Transient Laser Photochemistry

Picosecond Chemistry of Collisionless Molecules in Supersonic Beams By A.H. Zewail (With 4 Figures) 284

Energy Transfer in Picosecond Laser Generated Compressional Shock Waves. By A.J. Campillo, L.S. Goldberg, and P.E. Schoen (With 2 Figures) 289

The Role of A and A' States in the Geminate Recombination of Molecular Iodine. By D.F. Kelley and N.A. A.-Haj (With 4 Figures) 292

Molecular Dynamics of I_2 Photodissociation in Cyclohexane: Experimental Picosecond Transient Electronic Absorption. By P. Bado, C.G. Dupuy, J.P. Bergsma, and K.R. Wilson (With 3 Figures) 296

Iodine Photodissociation in Solution: New Transient Absorptions By M. Berg, A.L. Harris, J.K. Brown, and C.B. Harris (With 3 Figures) 300

Photodissociation of Triarylmethanes By L. Manring and K. Peters (With 4 Figures) 304

Femtosecond Time Resolved Multiphoton Ionization: Techniques and Applications. By B.I. Greene (With 8 Figures) 308

Threshold Ionization in Liquids By G.W. Robinson, J. Lee, and R.A. Moore (With 1 Figure) 313

Picosecond Multiphoton Laser Photolysis and Spectroscopy of Liquid Benzenes. By H. Miyasaka, H. Masuhara, and N. Mataga (With 3 Figures) 317

Chemical Reactions in Condensed Media By D. Statman, W.A. Jalenak, and G.W. Robinson (With 3 Figures) ... 320

Subpicosecond and Picosecond Time Resolved Laser Photoionization of Phenothiazine in Micellar Models. By Y. Gauduel, A. Migus, J.L. Martin, J.M. Lemaître, and A. Antonetti (With 2 Figures) 323

Isomerization Intermediates in the Photochemistry of Stilbenes By F.E. Doany and R.M. Hochstrasser (With 2 Figures) 326

Part VI Molecular Energy Redistribution, Transfer, and Relaxation

Picosecond Laser Studies on the Effect of Structure and Environment on Intersystem Crossing in Aromatic Carbenes. By E.V. Sitzmann, J.G. Langan, Z.Z. Ho, and K.B. Eisenthal (With 4 Figures) 330

Energy Flow from Highly Excited CH Overtones in Benzene and Alkanes
By E.L. Sibert III, J.S. Hutchinson, J.T. Hynes, and W.P. Reinhard
(With 7 Figures) 336

Pump-Pump Picosecond Laser Techniques and the Energy Redistribution
Dynamics in Mass Spectrometry. By M.A. El-Sayed, D. Gobeli, and
J. Simon (With 4 Figures) 341

Intramolecular Electronic and Vibrational Redistribution and Chemical
Transformation in Isolated Large Molecules - S_1 Benzene
By K. Yoshihara, M. Sumitani, D.V. O'Connor, Y. Takagi, and
N. Nakashima (With 5 Figures) .....

Ultrafast Intramolecular Redistribution and Energy Dissipation in
Solutions. The Application of a Molecular Thermometer
By P.O.J. Scherer, A. Seilmeier, F. Wondrazek, and W. Kaiser
(With 4 Figures) 351

Picosecond Time-Resolved Fluorescence Spectra of Liquid Crystal:
Cyanooctyloxybiphenyl. By N.Tamai, I. Yamazaki, H. Masuhara,
and N. Mataga (With 3 Figures) 355

Excited-State Solvation Dynamics in 4-Aminophthalimide
By S.W. Yeh, L.A. Philips, S.P. Webb, L.F. Buhse, and J.H. Clark
(With 3 Figures) 359

The Pyrazine Mystery: A Resolution
By A. Lorincz, F.A. Novak, D.D. Smith, and S.A. Rice
(With 1 Figure) 362

Picosecond Laser Studies of Photoinduced Electron Transfer in
Porphyrin-Quinone and Related Model Systems. By N. Mataga,
A. Karen, T. Okada, Y. Sakata, and S. Misumi (With 2 Figures) 365

The Excited-State Proton Transfer Reactions of Flavonols in Alcoholic
Solvents. By K.-J. Choi, B.P. Boczer, and M.R. Topp 368

Excited-State Proton-Transfer Reactions in 1-Naphthol
By S.P. Webb, S.W. Yeh, L.A. Philips, M.A. Tolbert, and J.H. Clark
(With 3 Figures) 371

Structural and Solvent Effects on the Excited State Dynamics of
3-Hydroxyflavones. By P.F. Barbara and A.J.G. Strandjord
(With 1 Figure) 374

Electron Transfer Reactions from the First Excited Singlet State of a
Polymethine Cyanine Dye. By D. Doizi and J.C. Mialocq
(With 3 Figures) 377

Photoinduced Electron Transfer in Polymethylene Linked Donor-Acceptor
Compounds: A-$(CH_2)_n$-D. By H. Staerk, W. Kühnle, R. Mitzkus,
R. Treichel, and A. Weller (With 2 Figures) 380

Four Wave Mixing Studies and Molecular Dynamics Simulations
By M. Golombok and G.A. Kenney-Wallace (With 1 Figure) 383

Relaxation of Large Molecules Following Ultrafast Excitation
By A. Lorincz, F.A. Novak, and S.A. Rice 387

Picosecond Time-Resolved Spectroscopy of Electronically Excited tris(2,2'-Bipyridine) Ruthenium(II) Dichloride. By L.A. Philips, W.T. Brown, S.P. Webb, S.W. Yeh, and J.H. Clark (With 3 Figures) .. 390

Part VII Electronics and Opto-Electronics

Modelocking at Ti:$LiNbO_3$-InGaAsP/InP Composite Cavity Laser Using a High-Speed Directional Coupler Switch. By R.C. Alferness, G. Eisenstein, S.K. Korotky, R.S. Tucker, L.L. Buhl, I.P. Kaminow, and J.J. Veselka (With 5 Figures) 394

Picosecond Optical Measurements of Circuit Effects on Carrier Sweepout in GaAs Schottky Diodes. By A. Von Lehmen and J.M. Ballantyne (With 4 Figures) 398

Color Center Formation and Recombination in KBr and LiF by Picosecond Pulsed Electrons. By K. Fujii, R. Kikuchi, S. Katagiri, K. Tsumori, and M. Kawanishi (With 4 Figures) 402

Subpicosecond Electro-Optic Sampling Using Coplanar Strip Transmission Lines. By K.E. Meyer and G.A. Mourou (With 2 Figures) 406

Čerenkov Radiation from Femtosecond Optical Pulses in Electro-Optic Media. By K.P. Cheung, D.H. Auston, J.A. Valdmanis, and D.A. Kleinman (With 5 Figures) 409

Ultraviolet Photoemission Studies of Surfaces Using Picosecond Pulses of Coherent XUV Radiation. By R. Haight, J. Bokor, R.H. Storz, J. Stark, R.R. Freeman, and P.H. Bucksbaum (With 3 Figures) 413

Synchronous Mode-Locking of a GaAs/GaAlAs Laser Diode by a Picosecond Optoelectronic Switch. By J. Kuhl and E.O. Göbel (With 3 Figures) . 417

Photochron Streak Camera with GaAs Photocathode By C.C. Phillips, A.E. Hughes, and W. Sibbett (With 4 Figures) 420

Sequential Waveform Generation by Picosecond Optoelectronic Switching By C.S. Chang, M.C. Jeng, M.J. Rhee, C.H. Lee, A. Rosen, and H. Davis (With 2 Figures) 423

Picosecond Gain Measurements of a GaAlAs Diode Laser By W. Lenth (With 3 Figures) 425

Transient Response Measurements with Ion-Beam-Damaged Si-on-Sapphire, GaAs, and InP Photoconductors. By R.B. Hammond, N.G. Paulter, and R.S. Wagner (With 2 Figures) 428

Picosecond Optoelectronic Studies of Microstrip Dispersion By D.E. Cooper (With 2 Figures) 430

Measurement of the Soft X-Ray Temporal and Spectral Response of InP:Fe Photoconductors. By D.R. Kania, R.J. Bartlett, P. Walsh, R.S. Wagner, R.B. Hammond, and P. Pianetta (With 1 Figure) 433

Dynamic Response of Millimeter Waves in a Semiconductor Waveguide to Picosecond Illumination. By A.M. Yurek, M.-G. Li, C.D. Striffler, and C.H. Lee (With 2 Figures) 436

Part VIII Photochemistry and Photophysics of Proteins, Chlorophyll, Visual Pigments, and Other Biological Systems

Time Resolution of Tryptophans in Myoglobin
By D.K. Negus and R.M. Hochstrasser (With 3 Figures) 440

Resolution of the Femtosecond Lifetime Species Involved in the Photodissociation Process of Hemeproteins and Protoheme. By J.L. Martin, A. Migus, C. Poyart, Y. Lecarpentier, A. Astier, and A. Antonetti (With 3 Figures) 447

Picosecond Vibrational Dynamics of Peptides and Proteins
By T.J. Kosic, E.L. Chronister, R.E. Cline, Jr., J.H. Hill, and D.D. Dlott (With 5 Figures) 452

New Investigations of the Primary Processes of Bacteriorhodopsin and of Halorhodopsin. By H.-J. Polland, W. Zinth, and W. Kaiser (With 2 Figures) 456

Primary Events in Vision Probed by Ultrafast Laser Spectroscopy
By A.G. Doukas, and R.R. Alfano (With 2 Figures) 459

Picosecond Time-Resolved Polarized Emission Spectroscopy of Biliproteins (Influence of Temperature and Aggregation)
By S. Schneider, P. Hefferle, P. Geiselhart, T. Mindl, F. Dörr, W. John, and H. Scheer (With 1 Figure) 462

Dynamics of Energy Transfer in Chloroplasts and the Internal Dynamics of an Enzyme. By R.J. Gulotty, L. Mets, R.S. Alberte, A.J. Cross, and G.R. Fleming (With 4 Figures) 466

Picosecond Single Photon Fluorescence Spectroscopy of Nucleic Acids
By R. Rigler, F. Claesens, and G. Lomakka (With 4 Figures) 472

Excited-State Dynamics of NADH and 1-N-Propyl-1,4-Dihydronicotinamide
By D.W. Boldridge, T.H. Morton, G.W. Scott, J.H. Clark, L.A. Philips S.P. Webb, S.M. Yeh, and P. van Eikeren (With 2 Figures) 477

Primary Process in the Photocycles of the Low pH Bacteriorhodopsin
By T. Kobayashi, H. Ohtani, J. Iwai, and A. Ikegami (With 2 Figures) 481

Picosecond Spectroscopy on the Primary Process in the Photoconversion of Protochlorophyllide to Chlorophyllide *a*. By T. Kobayashi, J. Iwai, M. Ikeuchi, and Y. Inoue (With 2 Figures) 484

Energy Transfer in Photosynthesis: The Heterogeneous Bipartite Model
By S.J. Berens, J. Scheele, W.L. Butler, and D. Magde 487

Excitation Energy Transfer in Phycobilin-Chlorophyll. A System of Algal Intact Cells. By I. Yamazaki, N. Tamai, T. Yamazaki, M. Mimuro, and Y. Fujita (With 2 Figures) 490

Analysis of Fluorescence Kinetics and Energy Transfer in Isolated α Subunits of Phycoerythrin from *Nostoc* Sp. By A.J. Dagen, R.R. Alfano, B.A. Zilinskas, and C.E. Swenberg (With 3 Figures) 493

Picosecond Time-Resolved Fluorescence Spectra of Hematoporphyrin Derivative and Its Related Porphyrins. By M. Yamashita, M. Nomura, S. Kobayashi, T. Sato, and K. Aizawa (With 1 Figure) 497

Femtosecond Spectrosopy of Bacteriorhodopsin Excited State Dynamics By M.C. Downer, M. Islam, C.V. Shank, A. Harootunian, A. Lewis (With 4 Figures) 500

Time-Resolved Picosecond Fluorescence Spectra of the Antenna Chlorophylls in the Green Alga Chlorella Vulgaris By J. Wendler, W. Haehnel, and A.R. Holzwarth (With 1 Figure) 503

Index of Contributors 507

Picosecond Time-Resolved Polarized Emission Spectroscopy of Biliproteins (Influence of Temperature and Aggregation)

S. Schneider, P. Hefferle, P. Geiselhart, T. Mindl, and F. Dörr

Institut für Physikalische und Theoretische Chemie, Technische Universität Lichtenbergstraße 4, D-8046 Garching, Fed Rep. of Germany

W. John and H. Scheer

Botanisches Institut der Universität, Menzingerstraße 67 D-8000 München, Fed. Rep. of Germany

1. Introduction

Phycobiliproteins are photosynthetic light-harvesting pigments in blue-green and red algae. They consist of 2-3 polypeptide subunits, each bearing up to 4 covalently bound linear tetrapyrrolic chromophores. In vivo the biliproteins are organized into complex structures, the phycobilisomes, which are attached to the outer thylakoid surface. Within the phycobilisome the excitation energy is transferred from the "outer" biliproteins with higher excitation energy to "inner" lying ones with lower excitation energy. In the intact alga the last step in the energy transfer chain leads to chlorophylls within the membrane, i.e. the reaction center. It is generally assumed that the energy transfer is based upon dipole - dipole interaction (Förster mechanism), but details are yet insufficiently understood. In an approach complementary to the study of energy transfer in functionally intact phycobilisomes or large fractions thereof (1), we are currently investigating by time-resolved fluorescence spectroscopy C-Phycocyanin (PC) isolated from Mastigocladus laminosus and its subunits, which are prepared according to procedures described earlier (2,3). All samples are dissolved in potassium phosphate buffer (80 mM, pH 6.0).

2. Measurements and Data Analysis

The fluorescence decay curves were measured using a synchronously pumped mode-locked ring dye laser (rhodamine 6G, 80 MHz repetition rate, pulse width $\leq$1 ps) in conjunction with a repetetively working streak camera (for details see, e.g., (4)). The apparent time resolution of this system is approximately 25 ps without deconvolution procedure; it allows measurements with low excitation intensities (10^{13} photons per pulse and cm^2). Fluorescence decay curves measured with the analyzer parallel, ($I_p(t)$), and orthogonal, ($I_s(t)$), to the polarization of the exciting beam are transferred to a minicomputer where, after proper correction for the systems response, the expressions $I(t) = I_p(t) + 2\,I_s(t)$ and $D(t) = I_p(t) - I_s(t)$ are calculated. I(t) measures the decay of the excited state population (electronic lifetime) and D(t) the product of the former with the correlation function of absorption and emission dipoles (2,5). In contrast to the anisotropy function R(t) the difference function D(t) is additive and can be evaluated if more than one emitting species is present. Lacking better information, we approximate the correlation function by an exponential. The best fits for both functions (I and D) are determined under the assumption of a biexponential response function (two emitting species) by means of a Marquardt algorithm.

Depending on the S/N ratio of the recorded fluorescence decay curves and their relative magnitude, the fit parameters derived may be subject to considerable error. We will, therefore, discuss their trends rather than their absolute magnitude.

3. Results and Discussion

It is found that in all cases the decay curves can be fitted sufficiently well as convolutions of biexponentials. The fit parameters, e.g., the decay times (T_1,T_2 in psec) and the relative amplitudes (A_1,A_2 in %) of the short- and long-lived component, resp., are given in the inserts in Fig. 1. The measurements were performed at three different temperatures, namely at 18° (A), at 36° (B), the temperature at which the algae are grown, and at 52° (C), where irreversible thermal denaturation starts to become effective. Partial denaturation takes place already at lower temperatures. Static measurements show a drastic loss in fluorescence yield (up to four orders of magnitude) which is much larger than the decrease in absorption connected with a conformational change of the chromophore (6). The time-integrated fluorescence intensities expressed as $A_1*T_1+A_2*T_2$ also confirm the reduction at higher temperature. It is found as a general rule that the decrease is more pronounced in the alpha than in the beta subunit and larger for the monomer than for the trimer. The normalized fluorescence decay curves show also small but distinct variations with temperature. For this reason the results presented in Fig. 1 must be taken as evidence for an intermediate state being present during the process of thermal denaturation.

The alpha subunit of PC contains only one chromophore. If it is stabilized by noncovalent interaction with the protein to adopt only one conformation, a single exponential decay is expected with a lifetime of 1.5 to 2.5 ns (lifetime of the chromophore in a native environment). Instead, an additional short-lived component is found, whose lifetime varies with temperature between 690 and 1060 psec. A similar behaviour was verified for the alpha subunit of Spirulina platensis (2) and Anabaena variabilis (7). Since aggregation of the subunits is unlikely, one must assume at least two different sets of emitting species, i.e. chromophore-protein-arrangements. The long-lived species must be close to that in native environment, whilst the short-lived form should be closer to the denatured, less interacting species. The faster decay in the difference function D(t), furthermore, signals that the faster component is subject to a depolarization mechanism with $T \simeq 1500$ psec. Since no acceptor molecules are present, the depolarization should be due to orientational relaxation of the less rigidly bound chromophores.

The beta subunit contains two chromophores in different protein environment. The respective absorption maxima are separated by about 20 nm. The stationary fluorescence spectra of both subunits are essentially equal, a fact which indicates an efficient energy transfer from the "sensitizing" to the "fluorescing" chromophore. The energy transfer is also manifested in the fluorescence decay curves. The short-lived component ($T_1 \simeq 300$ps) is interpreted as "leakage" fluorescence from the s chromophore, whose lifetime is shortened due to energy transfer to the f chromophore in the same subunit. The depolarization time of the fast component is much shorter than that of the alpha subunit and de-

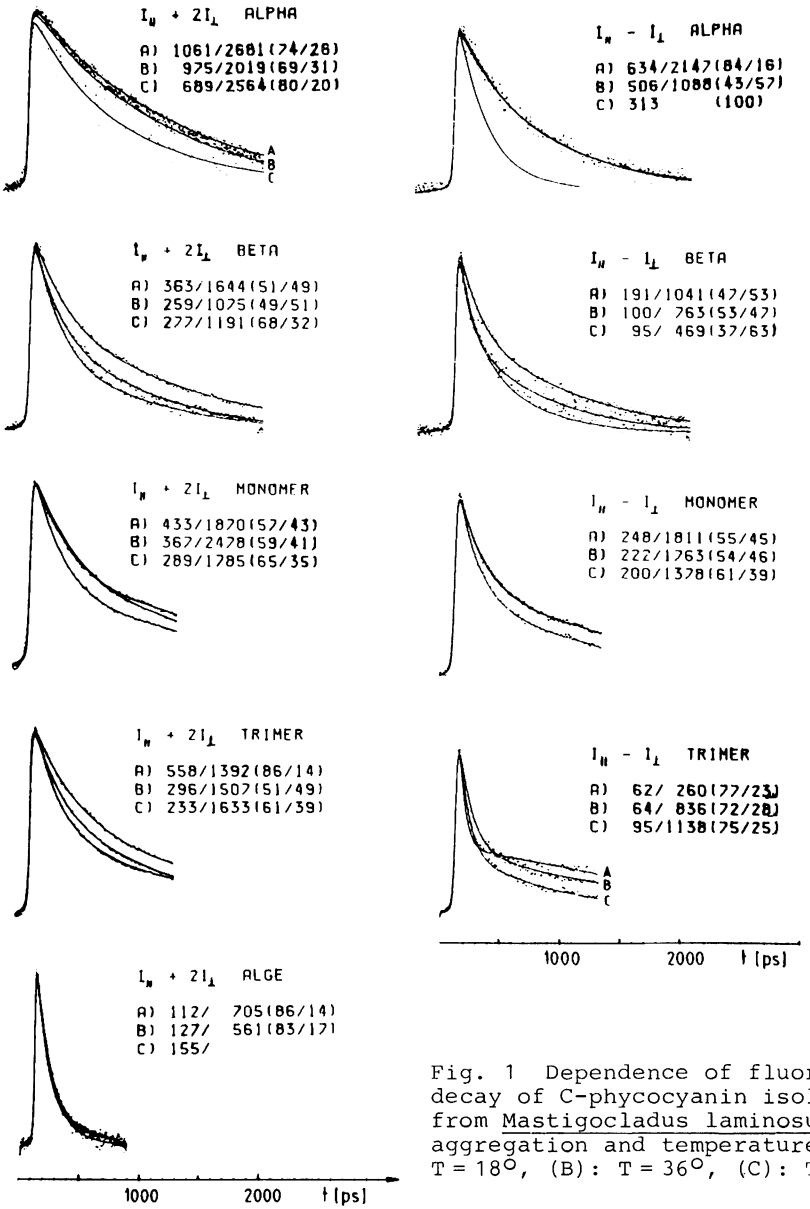

Fig. 1 Dependence of fluorescence decay of C-phycocyanin isolated from Mastigocladus laminosus on aggregation and temperature (A): T = 18°, (B): T = 36°, (C): T = 52°

creases with increasing temperature from 400 to 150 psec. The longer lifetime is close to the shorter one in the alpha subunit; a lifetime of 2 ns, which would be expected for the f chromophore in native environment is not detected, possibly for experimental reasons. An unambiguous interpretation is presently not possible, because different subsets of chromophore-protein arrangements can not be excluded in view of the preparation procedure which involves a denaturation - renaturation sequence.

The isotropic decay curves of monomers and trimers are similar to each other. The short lifetime is in the range of 200-600 psec and represents most likely the lifetime of the s chromophores, which are quenched by energy transfer.The longer one,which varies between 1600 and 2500 psec, characterizes the terminal acceptor, i.e. the f chromophore in the native environment. Chromophores excited via energy transfer rather than directly by photon absorption should emit a less polarized fluorescence. Only the short- lived leakage fluorescence is partly polarized, but the depolarization times are moderately short. In contrast to Spirulina platensis (2) we observe for PC from the thermophilic algae no significant increase of the depolarization time with temperature. In the intact alga, the energy is efficiently transferred to the nonfluorescing reaction center. The observed emission is only leakage fluorescence from PC and Allophycocyanin (APC). Since the fraction of emission from directly excited chromophores is small, the emission is essentially unpolarized.

References

1 For a recent review see,e.g.,"Biological events probed by ultrafast laser spectroscopy", ed. by R.R. Alfano (Academic Press, New York, 1982)
2 P. Hefferle, W. John, H. Scheer and S. Schneider, Photochem. Photobiol. 39,221 (1984)
3 W. Kufer, H. Scheer, Hoppe-Seyler´s Z. Physiol. Chem. 360,935 (1979)
4 P. Hefferle, M. Nies, W. Wehrmeyer, S. Schneider Photobiochem. Photobiophys. 5,41 (1983),id.5,325 (1983)
5 G.R. Fleming, J.M. Morris, G.W. Robinson, J.Chem.Phys. 17,91 (1976)
6 H. Scheer, H. Formanek, S. Schneider, Photochem.Photobiol. 36,259 (1982)
7 S.C. Switalski and K.Sauer, Photochem. Photobiol. in press